Journal of Applied Polymer Science

Novel Phenyl-POSS/Polyurethane Aqueous Dispersions and Their Hybrid Coatings

Jiankun Hu, Lian Li, Siwei Zhang, Linbo Gong, Shuling Gong
College of Chemistry and Molecular Sciences, Wuhan University, Wuhan 430072, China
Correspondence to: S. Gong (E-mail: gongsl@whu.edu.cn)

ABSTRACT: A facile and rapid preparation of 3-(2-aminoethylamino)propylheptaphenylPOSS (AA-POSS), a special phenyl-POSS that contains two functional amino groups (Scheme 1), is demonstrated by the corner-capping method. Then AA-POSS forms a series of novel phenyl-POSS/PU aqueous dispersions. The structure of AA-POSS has been confirmed by ^{1}H, ^{13}C, ^{29}Si NMR, and ESI-MS. The POSS/PU hybrid films are studied by Fourier transform infrared spectrometer (FT-IR), gel permeation chromatography (GPC), scanning electron microscope (SEM), X-ray diffraction (XRD) spectra, differential scanning calorimetry (DSC) analysis, and thermal gravimetric analyzer (TGA). FT-IR and GPC are conducted to validate the chemical structure of the hybrid PU. The properties of hybrid films display significant changes with notable increases in T_g, thermal properties, tensile strength, as well as surface hydrophobicity. These changes are attributed to the incorporation of novel POSS into PU. Moreover, these significant material property enhancements are achieved at low levels of POSS incorporation (only 4%). © 2013 Wiley Periodicals, Inc. J. Appl. Polym. Sci. 130: 1611–1620, 2013

KEYWORDS: applications; polyurethanes; properties and characterization; structure–property relations; thermogravimetric analysis (TGA)

Received 5 February 2013; accepted 19 March 2013; Published online 3 May 2013
DOI: 10.1002/app.39303

INTRODUCTION

Polyhedral oligomeric silsesquioxanes (POSS) comprise a class of important nanosized, cage-like molecules denoted by $[RSiO_{3/2}]_n$, where n is from 6 to 12 and R represents organic groups, one (or more) of which is reactive or polymerizable.[1] POSS are new fascinating materials in modern nanotechnology.[2] Nanostructured POSS are used as a class of precursors for synthesizing molecularly designed organic/inorganic hybrids. POSS can be incorporated into a polymer matrix through either mechanical melt blending or chemical functionalization of one or more functional groups into a corner of the POSS chemical structure. With molecular dimensions in the order of a single nanometer, POSS components not only bring the diversity but also make it easily compatible and well dispersed in organic polymers. Such nanoreinforced polymers significantly enhance the thermomechanical properties of materials while improving or retaining other physical properties, such as optical clarity, compatibility, and processability.[3]

Structure–property relationships in POSS, particularly the effects of different R groups to POSS and their modified polymers, are of particular interest.[4] Harrison described POSS as compounds composed of several Si—O linkages that forms a cage with different R substituents at its periphery. These R substituents are important because they determine various POSS physical and chemical properties.[5] In a separate experiment, phenyl-POSS (R = phenyl), bearing a phenyl functionality at the periphery, were discovered to be well-soluble in polymer systems, such as epoxy monomers. This characteristic is in contrast to isobutyl-POSS, which cannot be dissolved in an epoxy liquid even at small amounts.[6] Furthermore, POSS containing bulky phenyl groups at their periphery usually have better thermal stability, whereas isobutyl-POSS have excellent radiation resistance.[7,8] Considering the structural diversity and functional versatility of R substituents, certain desired properties, such as improved thermal decomposition, glass-transition temperatures (T_g), and mechanical properties, can be achieved by incorporating various POSS into polymer matrices.

A special field is represented by polyurethanes (PU), which is one of the most versatile polymeric materials used as adhesives, flexible films, coatings, or plastics. During the past decades, the growing environmental concerns, as well as health and safety risks, have pressed for the advancement of eco-friendly materials, thereby shifting technologies toward reducing or minimizing hazardous organic solvents to obtain aqueous polyurethane dispersions (PUDs). However, several properties of common PUD films, such as strength, water resistance, and heat resistance are lower than the solvent-based polyurethanes.[9] There are several ways to improve the properites of PUDs, such as crosslinking,[10] acrylic modifying mechod,[11] and UV curing technogloy[12] etc.

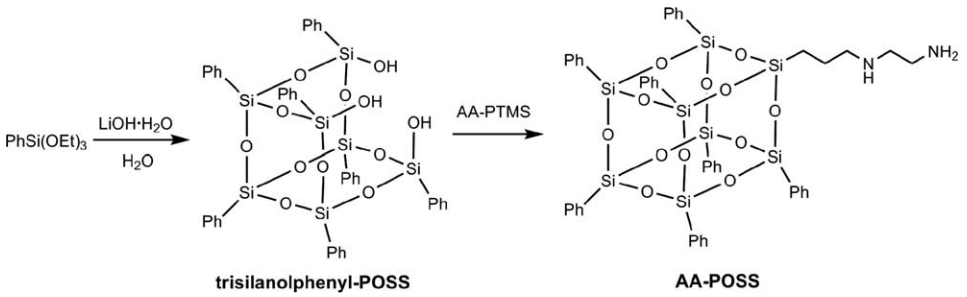

Scheme 1. The preparation of AA-POSS.

Utilizing POSS/PU hybrids is possibly a good approach for exploring the feasibility of new methods in improving these properties. Generally, POSS monomers with several functional groups are more suitable to be incorporated into PUD chains as chain extenders because these functional groups can easily react with isocyanates. Turri and Levi obtained a series of stable aqueous PUDs using a dihydroxy isobutyl-POSS (R = isobutyl) by the prepolymer mixing process.[13] In their work, surface hydrophobicity was significantly increased. However, no enhancement of the physical properties and thermal behavior of the polymers was found after the dried films were analyzed. Nanda et al. obtained diamino isobutyl-POSS grafted aqueous PUDs via the acetone process, in which the physical properties and surface properties of modified PUDs were enhanced as expected, but heat resistance was not significantly improved, even when more isobutyl-POSS were incorporated.[14] Moreover, the present POSS/PU hybrids are often limited to several POSS (mainly isobutyl-POSS) such that the more available POSS are rarely involved.[4] Hence, these limitations motivated us to develop novel POSS with excellent characteristics for enhancing the comprehensive properties of PUDs.

Phenyl-POSS have recently received considerable attention from organic synthesis to materials chemistry.[3] With the special R groups, phenyl-POSS exhibit more interesting and unique properties.[15] Zheng et al. used octaaminophenyl-POSS as crosslinking agents to react with PU prepolymers to form octa-armed, star-like POSS/PU hybrids.[16] The advantages of phenyl-POSS are readily apparent, as the finished polymer has been modified by it with excellent mechanical strength, heat resistance, oxidation resistance, and decreased flammability.[17] Moreover, if the enhanced properties are achieved, the levels of phenyl-POSS incorporation are far below the levels needed for traditional fillers.[18] Chen et al. demonstrated this concept in their work, in which the thermal and mechanical properties of hybrids were evidently enhanced after adding only a small amount of octaaminophenyl-POSS.[19] The water absorption concurrently significantly declined. However, either the preparation or the potential applications, there have been few reports about the practical exploitation of phenyl-POSS.

In this work, a facile and rapid preparation of 3-(2-aminoethylamino)-propylheptaphenylPOSS (AA-POSS), a special phenyl-POSS containing two functional amino groups (Scheme 1), is demonstrated by the corner-capping method. Then AA-POSS forms a series of novel phenyl-POSS/PU aqueous dispersions. Moreover, the thermal stability, physical property, and morphology of novel hybrids are discussed, and significant material property enhancements are achieved at low levels of POSS incorporation (only 4%).

EXPERIMENTAL

Materials

Hexamethylene diisocyanate (HDI), 2,2-bis(hydroxymethyl) butyric acid (DMBA), and poly(tetramethylene glycol), (PTMG, M_n = 2000) were purchased from Bayer Material Science (Pittsburgh, PA). The 3-(2-aminoethylamino) propyltrimethoxysilane (AA-PTMS) was provided by Hubei Diamond Advanced Material of Chemical (Hubei, China). Toluene, ethanol, di-*n*-butyltin dilaurate (DBTDL), triethylamine (TEA), 1,4-butanediol (BD), and tetrahydrofuran (THF) were received from Shanghai Regent Chemical (Shanghai, China). PTMG and DMBA were dried (80°C, 1 mmHg, 8 h) before use. BD was stored over dry molecular sieves. THF and toluene were refluxed and then distilled over sodium.

Synthesis of Trisilanolphenyl-POSS

Phenyltriethoxysilane (98.40 g, 0.41 mol) was added dropwise to $LiOH{\cdot}H_2O$ (8.48 g, 0.20 mol) and water (5.68 g, 0.32 mol) in an acetone/isopropanol (550 mL/100 mL) mixture at reflux. After maintaining the reaction mixture at this temperature for 24 h, it was cooled to room temperature, and then neutralized with 1 mol L^{-1} HCl (350 mL) while stirring for 2 h. The resulting solid was filtered and washed with distilled H_2O six times, and then air dried for 7 days. A 98% yield of trisilanolphenyl-POSS (59.30 g) was obtained. The selected characterization data for trisilanolphenyl-POSS were as follows: ^{1}H NMR (300 MHz, $CDCl_3$, 25°C) δ 7.86 (br, OH), δ 7.70 (br, OH), δ 7.48–7.60 (m, 14H, ArH), 7.13–7.38 (m, 21H, ArH); ^{13}C NMR (75 MHz, $CDCl_3$, 25°C) δ 134.10, 130.51, 130.30, 127.72; MS (ESI, CH_3OH): (m/z = 953, $[M+Na]^+$, 100%).

Synthesis of the AA-POSS

Trisilanolphenyl-POSS (50.00 g, 53.8 mmol) was dissolved in dry toluene (75 mL), followed by a dropwise addition of AA-PTMS (13.2 g, 59.2 mmol) at −8°C. Two drops of DBTDL were added as catalyst, and then the homogeneous solution was heated at room temperature for 12 h. The resulting solution and white precipitates were poured into a beaker containing 2 L of methanol, and the mixture was stirred for 2 h. The white precipitates were collected by vacuum filtration on a Buchner funnel, redissolved in 200 mL CH_2Cl_2, and filtered. Evaporation

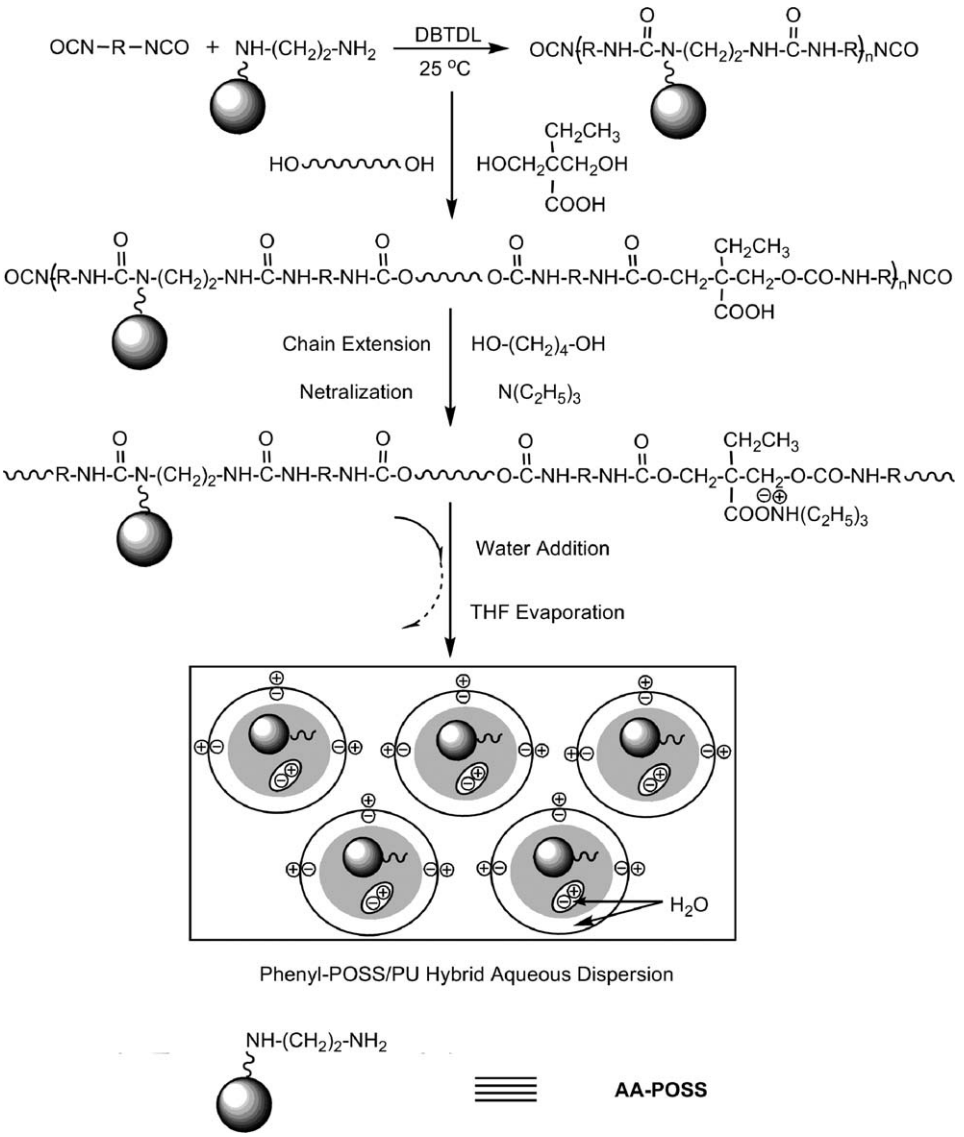

Scheme 2. The preparation of hybrids dispersions.

of the filtrate afforded the white solid and washed with acetonitrile twice. A total of 19.10 g (30%) of white precipitates were obtained. The selected characterization data for AA-POSS were as follows: ^{29}Si NMR (99.3 MHz, $CDCl_3$, 25°C) δ −64.94, −78.30, −78.73; ^{1}H NMR (300 MHz, $CDCl_3$, 25°C) δ 7.59–7.76 (m, 14H, ArH), 7.35–7.45 (m, 21H, ArH), 2.65 (t, 2H, CH_2, J = 6.0 Hz), 2.56 (t, 2H, CH_2, J = 6.6 Hz), 2.47 (t, 2H, CH_2, J = 6.0 Hz), 2.21 (br, 3H, NH), 1.62–1.69 (m, 2H, CH_2), 0.82 (t, 2H, CH_2, J = 7.6 Hz); ^{13}C NMR (75 MHz, $CDCl_3$, 25°C) δ 134.43, 131.02, 130.55, 128.12, 52.16, 49.63, 41.84, 23.27, 9.54; MS (ESI, CH_3OH): (m/z = 1057, $[M+H]^+$, 100%).

Representative POSS/PU Hybrid Preparation (PU12)

AA-POSS (12.00 g, 4.70 mmol) was dissolved into 120 g of dry THF contained in a 1-L round-bottom flask equipped with a mechanical stirrer and argon inlet. A total of 16.92 g of HDI (100.80 mmol) and four drops of DBTDL were added into the solution at room temperature. After 2 h, PTMG (62.08 g, 31.04 mmol) and DMBA (4.40 g, 29.70 mmol) were added into the flask under continuous stirring while the temperature was slowly raised to 65°C. The isocyanate (NCO) content was monitored according to the standard dibutylamine back-titration method.[20] Upon reaching the theoretical NCO value, the prepolymer chain was extended with BD (1.60 g, 17.58 mmol), and the reaction was continued for another 2 h to complete polymerization. TEA (3.00 g, 29.70 mmol) was finally added for neutralization, and the solution was stirred for 30 min while maintaining the temperature at 55°C. POSS/PU dispersion was attained by slowly adding water (220 g) to the neutralized acetone solution at 45°C with an agitation speed of 800 rpm. After stirring for 2 h, the reaction mixture was transferred to a rotary evaporator, and THF was removed at 40°C. Organic solvent-free dispersions with 30 wt % solids were obtained (Scheme 2).

The series of POSS/PU hybrid dispersions were synthesized by adding 4, 8, and 12% of POSS (by wt %). Neat PU (PU0) was

Table I. PU and Hybrid PU Compositions

Sample	AA-POSS wt (mmol)	HDI wt (mmol)	PTMG wt (mmol)	DMBA wt (mmol)	BD wt (mmol)	TEA wt (mmol)
PU0	0 (0)	16.00 (95.2)	75.00 (37.5)	4.4 (29.7)	1.6 (17.6)	3.0 (29.7)
PU4	4.0 (3.8)	16.32 (97.2)	70.68 (35.3)	4.4 (29.7)	1.6 (17.6)	3.0 (29.7)
PU8	8.0 (7.6)	16.60 (98.8)	66.40 (33.2)	4.4 (29.7)	1.6 (17.6)	3.0 (29.7)
PU12	12.0 (11.3)	16.92 (100.8)	62.08 (31.0)	4.4 (29.7)	1.6 (17.6)	3.0 (29.7)

also prepared and studied as control. The composition of the prepared POSS/PU hybrid is summarized in Table I.

Characterization

IR spectrum was recorded on a Fourier transform infrared (FT-IR) spectrometer (170SX, Nicolet, USA). Analyses were performed in the transmission mode in the range 4000–600 cm^{-1} at room temperature with a resolution of 2 cm^{-1} and accumulation of 16 scans. The molecular weights for the PU and POSS/PU samples were determined by GPC measurements in THF (Waters, GPCV-2000). The calibration was based on polystyrene standards, four different polystyrene standards of M_n = 178,700, 50,100, 9400, and 3060, were used to the calibration curve. The particle size and distribution of the waterborne polyurethane dispersion was measured using a Zetasizer Nano ZS (Malvern Instruments, UK). The viscosity of the dispersion was measured with a Brookfield LVDV-II viscometer (Middleboro, MA) at 25°C. The dispersions in sealed bottles were kept at room temperature to examine the storage stability. Contact angles were determined using a KRUSS DSA-100 contact angle meter employing distilled, deionized water as the reference liquid. About three independent measurements were carried out, and the average contact angle was reported. The tensile strength (σ_b) and elongation at break (b) of the dispersion-cast films were measured on a CMT6503 Universal Testing Machine (SANS, Shenzhen, China) at a crosshead rate of 100 mm min^{-1} according to ISO Standard 6239-1986. Differential scanning calorimetry (DSC) analysis was carried out on a DSC-204 instrument (Netzsch, Germany) under nitrogen atmosphere at a heating rate of 10°C min^{-1} in the range of −100–200°C. A Perkin–Elmer thermal gravimetric analyzer (TGA-7) was used to investigate the thermal stability of the hybrids. The samples (about 5 mg) were heated under a nitrogen atmosphere from ambient temperature up to 600°C at a heating rate of 10°C min^{-1}. XRD experiments were carried out on POSS powder and on 0.5-mm thick PU films with a Rigaku Ultima rotating anode X-ray generator (Rigaku Denki, Japan) using Cu Kα radiation source (=0.154 nm) at 40 kV and 60 mA with a scan rate of 6° min^{-1}. The diffraction angle of 2θ ranged from 5° to 40°. Scanning electron micrographs (SEM) observation was carried out on a Hitachi X-650 microscope (Mountain View, CA, Japan).

Films used for DSC, TG, XRD, and mechanical testing (40 × 10 × 0.80 mm^3) were prepared by casting onto a PTFE plate and drying in a vacuum oven at 40°C for 5 days. The water resistance of the films (40 × 20 × 0.80 mm^3) was measured by immersion of preweighed films in deionized water, respectively, for 24 h at room temperature. After the residual solvent was wiped from the film surface with filter paper, the weight of the swollen film was measured immediately. The swelling (solvent uptake) was expressed as the weight percentage of solvent in the swollen film:

$$\text{Swelling}(\%) = (W_s - W_d)/W_d \times 100\%$$

where W_s is the weight of the swollen film and W_d is the weight of the dry film.

RESULTS AND DISCUSSION

Structure

AA-POSS (Scheme 1) was confirmed by ^1H, ^{13}C, ^{29}Si NMR, and ESI-MS. The ESI-MS results proved the frank evidence that the target compound might be formed (m/z = 1057, $[M+H]^+$, 100%). ^1H and ^{13}C NMR analyses displayed peaks consistent with the desired product. ^{29}Si NMR analysis displayed three peaks at δ = −64.94, −78.30, −78.73 ppm (Figure 1), originating in a T structure present with a 1 : 4 : 3 ratio.[21]

Various amounts of AA-POSS were introduced into the PU networks. To compensate for the addition of POSS monomers, the PTMG content was reduced from 75 to 62 wt % of the total polymer solids as the AA-POSS content was varied from 0 to 12 wt % (Table I). When the AA-POSS content was >12 wt %, the films became too brittle or pale.

FTIR spectroscopy of AA-POSS, neat PU, and POSS/PU hybrids was conducted (Figure 2) to validate the POSS reaction with isocyanates. All isocyanates reacted because no NCO absorption appeared at 2270 cm^{-1}. For all PU samples, the free N—H group (3475 cm^{-1}) and hydrogen-bonded N—H group (3415 cm^{-1}) absorption peaks, which are the typical AA-POSS

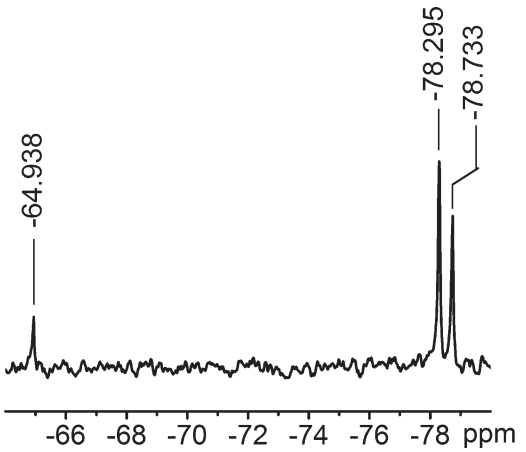

Figure 1. The ^{29}Si NMR of AA-POSS.

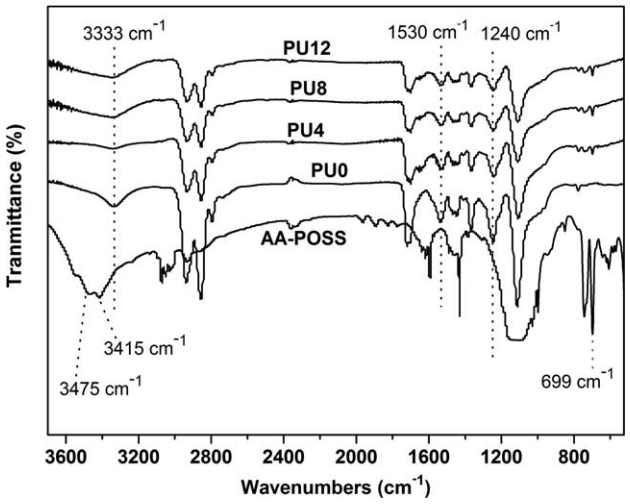

Figure 2. IR spectrum of AA-POSS and its hybrids.

peaks, were completely replaced by 3333–3340 cm^{-1} peaks (hydrogen-bonded N—H peak of urea/urethane).[22] The peak at 1530 cm^{-1} is assigned to the N—H bending vibration present in the PU samples, and the bands at ~1240 cm^{-1} can be collectively attributed to the ester C—O—C asymmetric stretching vibration.[23] The wide AA-POSS peak between 1078 and 1145 cm^{-1} is ascribed to Si—O stretching vibrations.[24] For the POSS/PU hybrids, this band unfortunately overlapped with that of the aliphatic ether. However, typical single substituent benzene peaks at 699 and 745 cm^{-1} are observed in both AA-POSS and POSS/PU hybrids, particularly in PU8 and PU12. These peaks indicate that POSS can be successfully incorporated into PU.

Table II shows the GPC traces of the molecular weights of all samples. The molecular weight of polymers slightly decreases with increasing POSS.[25]

Viscosity and Particle Size

In preparing aqueous PUDs, controlling viscosity and particle size with regard to the specific PUD application is important.[26] Particle size is governed by a number of internal and external factors, such as impeller speed, temperature, the concentration of polymer, ionic concentration, degree of neutralization, and hydrophilicity of the backbone. Among them and most important is the hydrophilicity of PU.[27] In the present PUDs, the DMBA content and other controlled factors are consistent. Therefore, the minor differences in particle size and viscosity with increasing POSS content indicate that adding AA-POSS monomers did not significantly affect the dispersion properties and dispersion step relative to PU0 (Table III). Moreover, the dispersion particle sizes of all the samples remained constant over 6 months of storage at room temperature.

Morphology

The films of conventional PU hybrids prepared with inorganic fillers or isobutyl-POSS were transparent, but the films of novel phenyl-POSS/PU hybrids were semi-transparent. This difference indicated that the phenyl-POSS were incompatible with PU systems, and phase separation or phase aggregates might occur. To improve the transparency of the hybrids, acetone, THF, acetone/toluene mixtures, and THF/toluene mixtures were chosen as the solutions in which to prepare the POSS/PU hybrids. During the reaction processes, all hybrid systems were homogeneous except for the acetone solution, which was probably due to the limited solubility of acetone and the excellent solubility of toluene. After curing completely, the films prepared in acetone appeared pale, and the others were semitransparent. Even the hybrid films prepared in pure toluene (without emulsification, and the solution was directly cast on the PTFE plates) were also semitransparent. Therefore, we failed to improve the transparency of the hybrids. Further experiments on improving their transparencies are in process.

The XRD spectra of the PU films were measured and are shown in Figure 3. The unreacted AA-POSS monomers have well-defined reflections at $2\theta = 7.30°$, 8.64°, 9.30°. Using Bragg's equation, $2d\sin\theta = k\lambda$, the following corresponding space values (d) were obtained: 12.09, 10.22, and 9.50 Å. Such results are consistent with the hexaphenylhexasilsesquioxane structure reported by Barry.[28] Unfortunately, determining the AA-POSS crystalline structure also failed (similar to hexaphenylhexasilsesquioxane) because of the same difficulty of growing crystals suitable for a single crystal X-ray analysis. However, all POSS/PU hybrids exhibit slight residual crystallinity with a broad peak at about 8.5°, even though PU4 exhibited low peak intensity. This fact would mean that AA-POSS cages maintain a relevant self-assembling ability even when copolymerized by a predominantly statistical process, with formation of nanocrystal phases.

Water Resistance

As expected, incorporating the POSS comonomers significantly affects the film surfaces, as shown by the large changes in water uptake and contact angle (Table III). POSS/PU films systematically show a lower water uptake with the POSS content. As POSS content increased from 0 to 4.0 wt %, water uptake decreased from 13.6 to 3.2%. It is possible that the POSS migrated onto the surface, thereby preventing the solvent molecules from entering the bulk. Moreover, POSS are highly hydrophobic so the water uptake of the hybrid films was much lower than that of pure PU0 film. Incorporating 4 wt % POSS (PU4) increased the contact angle from 62° to 91°, and higher loadings slowly increased the contact angle to 95°. This phenomenon is consistent with others POSS modified polymers as surface tension preferentially drives the lower energy POSS residues to the air interface.[29]

Mechanical Properties

Initial tensile tests on the films prepared from the series also indicated significant changes with the inclusion of POSS (Table III). Mechanical properties changed systematically with the

Table II. GPC of the Hybrids

Sample	M_w (GPC)	M_n (GPC)	PDI = M_w/M_n
PU0	32,010	26,025	1.23
PU4	28,892	24,694	1.17
PU8	25,424	20,839	1.22
PU12	21,224	18,782	1.13

Table III. Physical Properties of the Hybrids

Sample	Particle size (nm)	Viscosity (mPa·s)	Contact angle (deg)	Tensile strength at break (MPa)	Elongation at break (%)	Water uptake (%)
PU0	80	76	62 ± 2	1.34	1230	13.6
PU4	85	75	91 ± 2	1.92	1200	3.2
PU8	87	72	94 ± 2	2.75	1140	2.6
PU12	90	71	95 ± 2	3.63	1050	2.1

POSS content. The tensile strength at break increased with the POSS content from 1.34 MPa for the PU0 to 3.62 MPa for the samples containing 12% of the POSS monomers (Figure 4). Concurrently, there is a slightly drop in elongation at break, though the stiffest films with 12% POSS still attained 1050% elongation before breaking. The rigidity of the hybrids clearly increased with the POSS content, thereby increasing the tensile strength and lowering the elongation at break.

The tensile fracture surfaces of PU films are shown in Figures 5 and 6. Figure 5 shows the SEM micrographs of PU0 and PU12. The micrographs of the other POSS loadings are similar to that of PU12, and thus, are not shown. The magnified micrographs of all samples are shown in Figure 6. The fracture of the neat PU is smooth because of quick or brittle failure.[30] However, adding POSS roughens the crack surface, indicating that the roughness increases as the POSS content increases. The fracture roughness indicates that a strong resistance to the crack propagation and that the crack does not easily propagate, in contrast to that in neat PU.[31] The fracture surface roughness indicates a large crack propagation and increased torturous path of the propagating crack.[32] It is likely that this effect improved the strength of the hybrids. Furthermore, the fracture surface of PU4 is quite different from those of PU8 and PU12, in which the fracture surfaces become rougher with large cracks (Figure 6). This behavior further indicates that POSS do not peel off from materials as cracks propagate, and that the bonding between PU and POSS is very strong.

The changes in physical properties, including the subsequent T_g, are consistent with the expected changes with an increase in hard segment content of PU and with the first-order estimates of the hard segment content as the amount of POSS is increased. The simple estimates for this polymer series are listed in Table IV. These estimates were made with the assumption that the soft segment content comprises PTMG and the molar equivalents of HDI its react with. Others are considered as hard segment contents. Transitioning into the PU soft segment phase would generally decrease the soft segment content from 81.3 to 67.3 wt % as the POSS level increased to 12% of the total composition, whereas the total hard segment content would increase from 18.7 to 32.7 wt %. The subsequent thermal gravimetric analysis (TGA) was almost consistent with this theoretical computation, indicating that this assumption is reasonable. The slight differences resulted from the effect of POSS. The detailed experimental mass loss data are presented in Table IV.

Thermodynamics

Differential scanning calorimetry (DSC) provides information regarding transition temperatures, such as the T_g and melting temperature (T_m), as well as the degree of phase separation. Figure 7 illustrates the DSC curves of the series of aqueous POSS/PU hybrid films. PU0 exhibits apparent melting endotherms at 18.3°C, which corresponds to the T_m of microcrystallites or crystals.[33] That peaks of the hybrids decline when the POSS content increases, indicating that adding phenyl-POSS disrupts intermolecular chain packing, thereby preventing crystallization.[34,35] A hard segment T_g was observed in the higher temperatures (Table V). T_g increased from 75 to 99°C as the POSS content increased from 0 to 12 wt %. From the man-made dotted line in Figure 7, the trend of T_g is shown clearly.

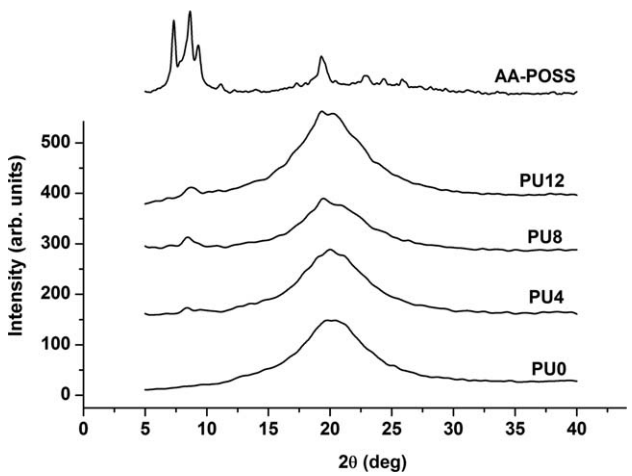

Figure 3. XRD curves of the hybrid films.

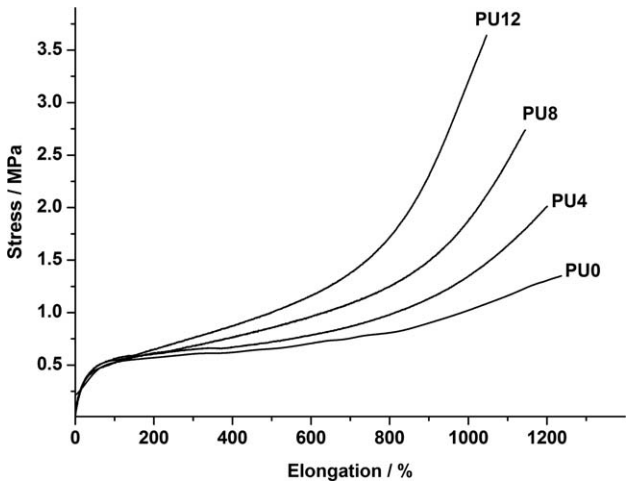

Figure 4. Tensile tests of hybrids.

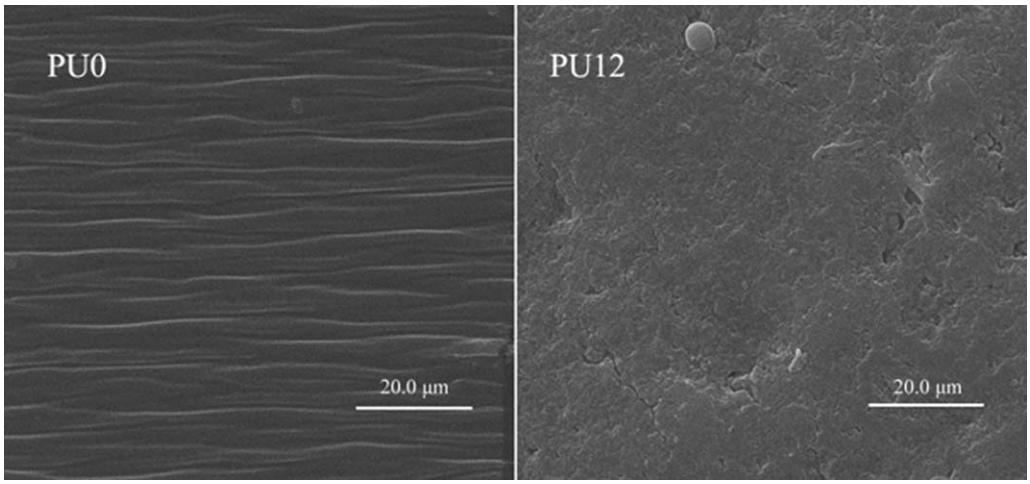

Figure 5. SEM of PU0 and PU12.

Similar results and phenomenon were also observed in the other POSS/PU matrices.[36] Considering the nanophase dispersion, rigid phenyl groups, and chemical incorporation to PU chains of phenyl-POSS, these factors effectively hindered the PU chain motions. Thus, the T_g of the matrix increased.[37]

The thermal properties of all films were examined by TGA to investigate the improvement of PU systems with phenyl-POSS incorporation. Under a nitrogen atmosphere, a two-step thermal degradation of PU occurred (Figure 8). The first degradation step that began at ~270°C regardless of the POSS concentration was mainly due to the degradation of hard segments.[38,39] The second step corresponded to the thermal decomposition of soft segments between 350 and 480°C.

Although the very minor differences in degradation temperature, T_d, (10% mass loss) indicated that the POSS monomers did not significantly affect the initial T_d, the T_d of PU12 was

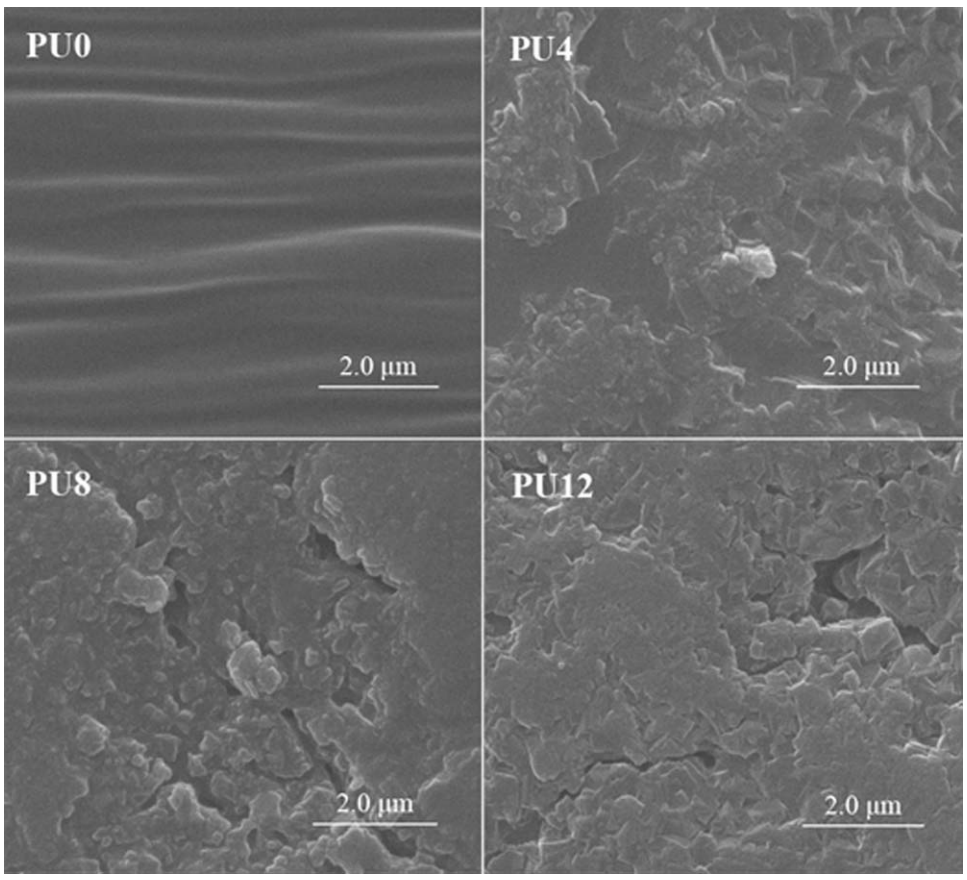

Figure 6. The magnification of SEM of all films.

Table IV. Calculated Weight Percent and Experimental Mass Loss Percent

Sample	Hard segment calculational content (%)	Soft segment calculational content (%)	Hard segment mass loss (%) N_2	Soft segment mass loss (%) N_2	Hard segment mass loss (%) air	Soft segment mass loss (%) air
PU0	18.7	81.3	17.9	82.1	17.4	82.6
PU4	23.4	76.6	23.1	73.1	22.9	73.5
PU8	28.0	72.0	24.9	68.8	24.8	68.0
PU12	32.7	67.3	25.7	63.5	25.1	64.2

delayed from 294°C (PU0) to 297°C. However, the mass losses at the first degradation step were much different. The important characteristics are summarized in Table IV. For instance, the mass losses for PU0, PU4, PU8, and PU12 were 17.9, 23.1, 24.9, and 25.7 wt %, respectively. PU12 had the highest loss among all these hybrids. In the second degradation step, the highest weight losses occurred between 350 and 480°C, and the mass losses for PU0, PU4, PU8, and PU12 were 82.1, 73.1, 68.8, and 63.5 wt %, respectively. The characteristic temperatures of PU0, PU4, PU8, and PU12 for a 50% weight loss were 390, 409, 416, and 423°C, respectively. In either the first or second degradation step, the weight loss rate decreased as the POSS content increased. The T_d of ether bonds increased approximate 30°C from 350°C (a small hump for PU0 around this temperature was observed in Figure 9, which probably implied the initial degradation of ether bonds) to 380°C. Similar results were also observed for the other PU hybrids, but their increments were generally not larger than 10°C.[40] Moreover, the temperatures of the maximum peak (T_{max}) degradation were delayed from 403°C (PU0) to 416°C (PU4), whereas the characteristic yield improved from 0 to 3.8% at 600°C (Table V). Higher loadings (PU12) increased the T_{max} to 420°C and the characteristic yield to 10.8%. Interestingly, the T_{max} and characteristic yield varied systematically with the POSS content. Therefore, phenyl-POSS significantly improves the thermal stability of PU, particularly at high temperatures.

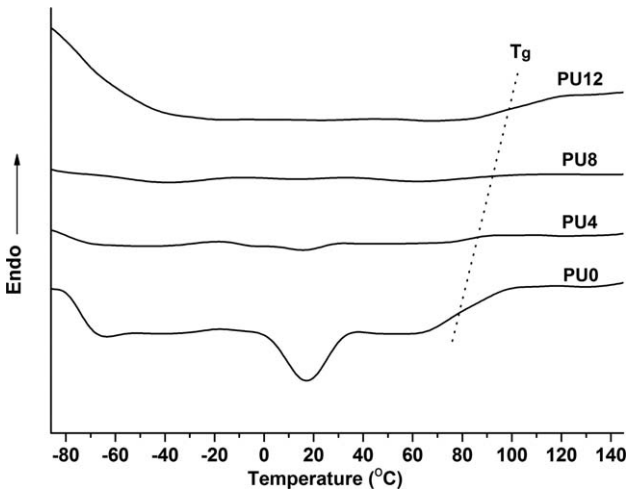

Figure 7. DSC curves of the hybrid films.

The thermo-oxidative properties of all films were also examined. As shown in Figure 10, the thermo-oxidative behavior was more complex than the thermal degradation behavior under a nitrogen atmosphere; three degradation steps were observed. The mass losses in the first degradation step at approximately between 250 and 350°C ranged from 18 to 25%. The greatest weight loss occurred in the second degradation step between 350 and 440°C. The third degradation step, which started at ~440°C and ended at 600°C, had a total weight loss of about 14%.

The thermo-oxidative stability of POSS/PU hybrids increased with the POSS content. For instance, the T_d of PU0, PU4, PU8, and PU12 were 285, 297, 303, and 307°C, respectively. PU12 had the highest T_d among all these hybrids. The T_d of the hybrids increased slightly, with a maximum increase of about 22°C from 285 to 307°C with the increasing POSS content from 0 to 12 wt %. The characteristic temperatures of PU0, PU4, PU8, and PU12 for the 50% weight loss were 393, 415, 422, and 424°C, respectively (Table V). At 600°C, the neat PU was completely degraded without any inert residue remaining, whereas the PU4, PU8, and PU12 residues were 3.6%, 7.2%, and 10.7%, respectively. These results were similar to the residues under a nitrogen atmosphere. In the last degradation step, ~14% mass loss for all the samples was observed between 440 and 600°C. Hence, the decomposition products also affected the last degradation rate and O_2 consumption because both the second and the third steps corresponded to the thermal decomposition of the soft segments,[39] thereby causing the 14% mass loss. Similar results were also found in previous reports.[41] However, the beginning of the degradation temperature for this step in the current study was much different, and the temperatures of PU0, PU4, PU8, and PU12 were 437, 449, 458, and 460°C, respectively, with the PU12 temperature much higher by about 23°C compared with that of PU0. These values suggested that the PU films with more POSS are more stable.

Therefore, phenyl-POSS could be developed as a novel thermal resistive material, as illustrated by the TGA (Figure 11). The initial T_d of phenyl-POSS was 502°C (nitrogen atmosphere), at which PU0 was completely degraded, even though at 800°C the POSS still retained 70% residues. Under an air atmosphere, the initial T_d was 457°C, which was lower than that under nitrogen atmosphere, but still higher than the T_d of PU0 (285°C). Furthermore, the POSS residue at 800°C was ~45.0%, which was highly consistent with the theoretical value of silicon dioxide (45.5%). Similar results were also found in previous reports, in

Table V. Thermodynamic Properties of the Hybrid Films

Sample	Hard segment T_g	Temperature of 50% mass loss N_2	Temperature of 50% mass loss air	Temperature of peak degradation N_2	Residue (%) at 600°C N_2	Residue (%) at 600°C air
PU0	75	390	393	403	0	0
PU4	80	409	415	416	3.8	3.6
PU8	87	416	422	418	6.3	7.2
PU12	99	423	424	420	10.8	10.2

which the white residues were commonly regarded as silicon dioxide that were formed in the thermal-oxidative degradation process of POSS.[15,36]

The increased effect for hybrids can be explained in two ways. On the one hand, according to the Vyazovkin model,[42] the enhancement of the thermal stability of POSS/PU polymers is caused by the suppression of the molecular mobility of polymer chains by bulky phenyl-POSS.[43] Considering that molecular mobility mainly contributes to the transport of reactive species within the polymer, nanocomposites are likely to have lower reactivities, and, therefore, greater chemical and thermal stabilities than neat PU.[40,44] On the other hand, chemically incorporated phenyl-POSS groups (or POSS agglomerates) provides additional heat capacities, thereby stabilizing the bulk materials against thermal decomposition.[45,46] This stabilization improves thermal stability as well.

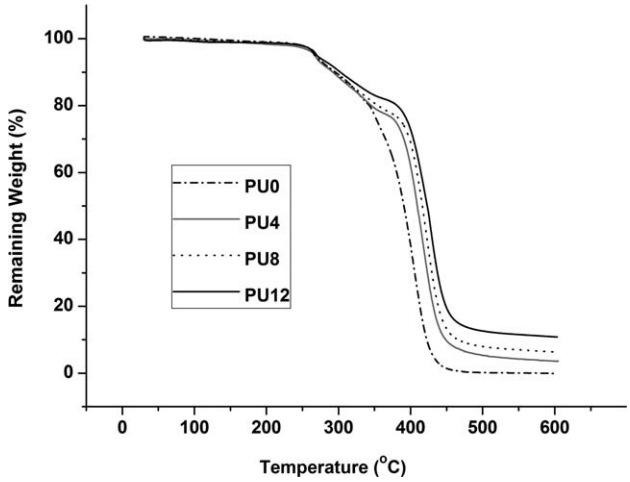

Figure 8. TG curves of the hybrid films (nitrogen atmosphere).

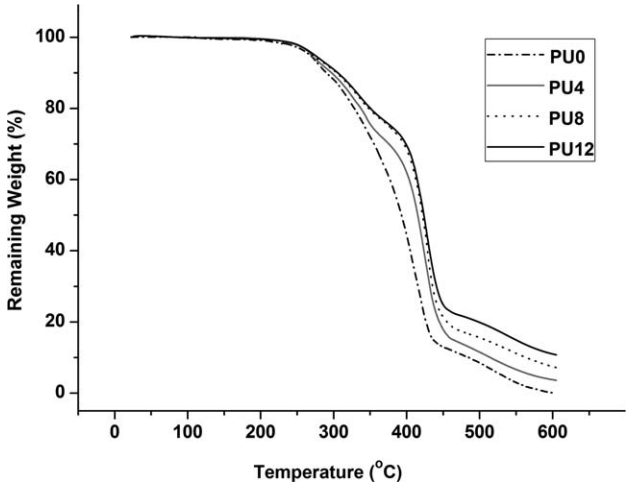

Figure 10. TG curves of the hybrid films (air atmosphere).

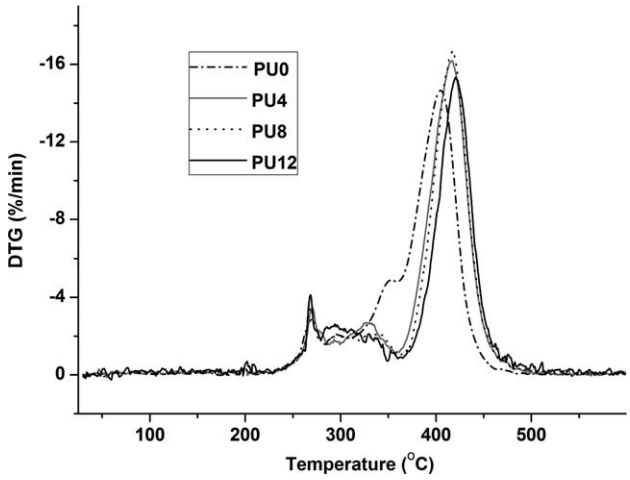

Figure 9. DTG curves of the hybrid films (nitrogen atmosphere).

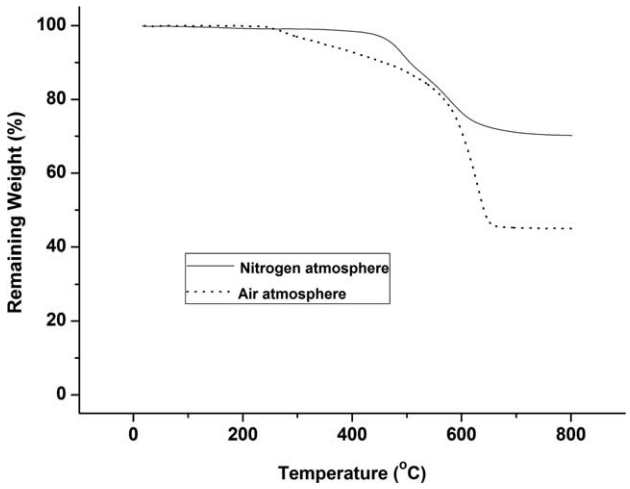

Figure 11. TG curves of AA-POSS (N_2 atmosphere and air atmosphere).

CONCLUSION

Novel aqueous PUDs were synthesized from new phenyl-POSS using the corner-capping method. The exact structure of these PUDs was validated by NMR and ESI-MS. All dispersions were stable for more than 6 months and contained little or no volatile organic compounds. Incorporating phenyl-POSS (only 4 wt %) can prominently enhance the mechanical and thermal properties of PU, and this low-level POSS incorporation exhibits the advantages of the phenyl-POSS. Overall, this study effectively reports the feasibility of preparing phenyl-POSS/PU dispersions with remarkable reproducible properties for diverse potential applications, including electronic devices, coatings, adhesives, and actuators.

ACKNOWLEDGMENTS

The authors are grateful to the National Natural Science Foundation of China (20772092) and the Hubei Province Natural Science Fund for Distinguished Young Scholars (2007ABB021) for financial support.

REFERENCES

1. Ni, Y.; Zheng, S. X. *J. Polym. Sci. A Polym. Chem.* **2007**, *45*, 1247.
2. Wang, F. K.; Lu, X. H.; He, C. B. *J. Mater. Chem.* **2011**, *21*, 2775.
3. Tanaka, K.; Chujo, Y. *J. Mater. Chem.* **2012**, *22*, 1733.
4. Cordes, D. B.; Lickiss, P. D.; Rataboul, F. *Chem. Rev.* **2010**, *110*, 2081.
5. Harrison, P. G. *J. Organomet. Chem.* **1997**, *542*, 141.
6. Fu, B. X.; Namani, M.; Lee, A. *Polymer* **2003**, *44*, 7739.
7. Hu, J. K.; Zhang, Q. C.; Gong, S. L. *Chin. Chem. Lett.* **2012**, *23*, 181.
8. Spoljaric, S.; Genovese, A.; Shanks, R. A. *J. Appl. Polym. Sci.* **2012**, *123*, 585.
9. Asif, A.; Shi, W. F. *Polym. Adv. Technol.* **2004**, *15*, 669.
10. Lee, J. S.; Kim, B. K. *J. Appl. Polym. Sci.* **2001**, *82*, 1315.
11. Pilch-Pitera, B. *J. Appl. Polym. Sci.* **2012**, *123*, 807.
12. Yang, Z. L.; Wicks, D. A.; Yuan, J. J.; Pu, H. T.; Liu, Y. S. *Polymer* **2010**, *51*, 1572.
13. Turri, S.; Levi, M. *Macromolecules* **2005**, *38*, 5569.
14. Nanda, A. K.; Wicks, D. A.; Madbouly, S. A.; Otaigbe, J. U. *Macromolecules* **2006**, *39*, 7037.
15. Roll, M. F.; Kampf, J. W.; Kim, Y.; Yi, E.; Laine, R. M. *J. Am. Chem. Soc.* **2010**, *132*, 10171.
16. Liu, H. Z.; Zheng, S. X. *Macromol. Rapid. Commun.* **2005**, *26*, 196.
17. Song, J. X.; Chen, G. X.; Wu, G.; Cai, C. H.; Liu, P. G.; Li, Q. F. *Polym. Adv. Technol.* **2011**, *22*, 2069.
18. Madbouly, S. A.; Otaigbe, J. U. *Prog. Polym. Sci.* **2009**, *34*, 1283.
19. Chen, G. X.; Si, L. X.; Lu, P.; Li, Q. F. *J. Appl. Polym. Sci.* **2012**, *125*, 3929.
20. Nanda, A. K.; Wicks, D. A. *Polymer* **2006**, *47*, 1805.
21. Wheeler, P. A.; Fu, B. X.; Lichtenhan, J. D.; Jia, W. T.; Mathias, L. J. *J. Appl. Polym. Sci.* **2006**, *102*, 2856.
22. Mattia, J.; Painter, P. *Macromolecules* **2007**, *40*, 1546.
23. Lee, H. T.; Hwang, J. J.; Liu, H. J. *J. Polym. Sci. A Polym. Chem.* **2006**, *44*, 5801.
24. Wypych, F.; Schreiner, W. H.; Mattoso, N. D.; Mosca, H.; Marangoni, R.; Bento, C. A. D. *J. Mater. Chem.* **2003**, *13*, 304.
25. Iyer, S.; Schiraldi, D. A. *Macromolecules* **2007**, *40*, 4942.
26. Wen, T. C.; Wang, Y. J.; Cheng, T. T.; Yang, C. H. *Polymer* **1999**, *40*, 3979.
27. Mohaghegh, S. M. S.; Barikani, M.; Entezami, A. A. *Colloids Surf. A* **2006**, *276*, 95.
28. Barry, J.; Daudt, W. H.; Domicone, J. J.; Gilkey, J. W. *J. Am. Chem. Soc.* **1955**, *77*, 4248.
29. Tan, J. J.; Jia, Z. Y.; Sheng, D. K.; Wen, X.; Yang, Y. M. *Polym. Eng. Sci.* **2011**, *51*, 795.
30. Subramani, S.; Lee, J. Y.; Choi, S. W.; Kim, J. H. *J. Polym. Sci. B Polym. Phys.* **2007**, *45*, 2747.
31. Subramani, S.; Choi, S. W.; Lee, J. Y.; Kim, J. H. *Polymer* **2007**, *48*, 4691.
32. Wu, C. L.; Zhang, M. Q.; Rong, M. Z.; Friedrich, K. *Compos. Sci. Technol.* **2002**, *62*, 1327.
33. Yang, D. Y.; Hu, C. P.; Ying, S. K. *J. Polym. Sci. A Polym. Chem.* **2005**, *43*, 2606.
34. Paik Sung, C. S.; Hu, C. B.; Wu, C. S. *Macromolecules* **1980**, *13*, 111.
35. Markovic, E.; Ginic-Markovic, Clarke, M. S.; Matisons, J.; Hussain, M.; Simon, G. P. *Macromolecules* **2007**, *40*, 2694.
36. Wang, H. H.; Lin, Y. T. *J. Appl. Polym. Sci.* **2003**, *90*, 2045.
37. Fu, B. X.; Gelfer, M. Y.; Hsiao, B. S.; Phillips, S.; Viers, B.; Blanski, R.; Ruth, P. *Polymer* **2003**, *44*, 1499.
38. Bourbigot, S.; Turf, T.; Bellayer, S.; Duquesne, S. *Polym. Degrad. Stab.* **2009**, *94*, 1230.
39. Chattopadhyay, D. K.; Webster, D. C. *Prog. Polym. Sci.* **2009**, *34*, 1068.
40. Janowski, B.; Pielichowski, K. *Thermochim. Acta* **2008**, *478*, 51.
41. Servay, T.; Voelkel, R.; Schmiedberger, H.; Lehmann, S. *Polymer* **2000**, *41*, 5247.
42. Vyazovkin, S.; Dranca, I.; Fan, X. W.; Advincula, R. *J. Phys. Chem. B* **2004**, *108*, 11672.
43. Wu, C. S.; Liu, Y. L.; Hsu, K. Y. *Polymer* **2003**, *44*, 565.
44. Zhang, H. Q.; Farris, R. J.; Westmoreland, P. R. *Macromolecules* **2003**, *36*, 3944.
45. Zuo, M.; Takeichi, T. *Polymer* **1999**, *40*, 5153.
46. Vaia, R. A.; Maguire, J. F. *Chem. Mater.* **2007**, *19*, 2736.